Journal of Biological Methods | **2020** | **Vol**. 7(4) | e141
DOI: 10.14440/jbm.2020.334

BENCHMARK

Comparison of different clearing and acquisition methods for 3D imaging of murine intestinal organoids

Louison Lallemant[1], Corinne Lebreton[2], Meriem Garfa-Traoré[1]*

[1]Cell Imaging Platform, INSERM-US24-CNRS UMS 3633 Structure Fédérative de Recherche Necker, Paris University, Paris 75015, France
[2]Université de Paris, Imagine Institute, Laboratory of Intestinal Immunity, INSERM UMR1163, Paris 75015, France

*Corresponding author: Meriem Garfa Traore, Email: meriem.garfa@inserm.fr

Competing interests: The authors have declared that no competing interests exist.

Abbreviations used: BSA, bovin serum albumin; DMEM, Dulbecco's modified eagle medium; FBS: foetal bovine serum; LSM: laser scanning microscopy; OC, OptiClear; PBSO, phosphate buffer saline without calcium; PFA, paraformaldhehyde; RC, RapiClear; SI, small intestine; TDE, 2,2′-thiodiethanol; 3D, three dimensions

Received April 20, 2020; Revision received August 17, 2020; Accepted August 17, 2020; Published December 28, 2020

ABSTRACT

An organoid is a three-dimensional multicellular structure that shows realistic micro-anatomy of an organ. This *in vitro* model mimics the *in vivo* environment, architecture and multi-lineage differentiation of the original organs and allows to answer many interesting biological questions. For these reasons, they are widely used in stem cell, regenerative medicine, toxicology, pharmacology, and host-microbe interactions research. In order to study organoids, microscopy is very useful: It is possible to make three-dimensional reconstruction of serial sections but it is time consuming and error-prone. Here we propose an alternative solution: Tissue clearing reduces the dispersion of light because it homogenizes the refractive index of the tissue, allowing sample observation throughout its thickness. We have compared different clearing techniques on mouse intestinal organoids using different acquisition methods.

Keywords: clearing, intestinal organoids, three-dimension imaging

INTRODUCTION

Today we know how to create *in vitro* a "mini-organ" called "organoid" [1]. Organoid models have been developed for a large number of organs including the intestine [2,3]. These biological tools tend to become essential and allow major advances in biology and medicine. Importantly, these *in vitro* 3D models can mimic what happens in the whole organ.

For example, recent studies have shown that organoids can be used as an alternative to animal models to study diseases [4]. Organoids can be combined with CRISPR/Cas9 technique to study the genetic basis of diseases [5]. Using organoids, it is also possible to study host-pathogens interactions [6,7], to understand physiological processes [4,8] and to analyze the mechanisms involved in development [9]. Finally, organoids can also provide an important source of cells and tissues for grafting and cell therapy techniques [5,10].

In this context, immunofluorescence microscopy is essential to visualize biological structures and organisms in 3D. Usually the methodology implies previous sectioning of the tissue, followed by 3D reconstruction of serial sections. This procedure is time-consuming and is subject to errors, especially due to artifacts introduced by cutting and the difficulty to stitch the images.

Over the past few years, we have seen the emergence of many clearing techniques, many developed by neuroscientists in order to study the brain in its entirety [11]. These techniques are now used to study various organs: kidney, spleen, liver, heart and even the whole mouse. Clearing can also be used on organoids of different origins [12]. In order to image a thick sample throughout its thickness, it is necessary to reduce the dispersion of light by homogenizing the refractive index of the tissue [13]. There are different approaches to achieve this goal: either by simple immersion of the sample in an aqueous medium, or by delipidation and dehydration in an organic or aqueous solvent [14]. Tissue clearing techniques have resulted in the observation of thick specimens and even whole organisms without the use of sectioning. Thus, 3D imaging of a large sample with high resolution is now possible [15].

Here we first provide a comparison of four easy, quick and inexpensive clearing methods for 3D imaging of murine intestinal organoids: (1) TDE: a clearing method based on the use of 2,2'-thiodiethanol, a glycol derivative previously reported as a mounting medium to adjust sample's refractive index (RI) and used to clear thick samples [16], (2) Opticlear: a clearing method developed for human brain slice clearing [17], (3) CUBIC: a widely used clearing method given its simplicity, low cost and good preservation of fluorescent proteins [18] and (4) RapiClear 1.47: a technique based on a commercial clearing solution

How to cite this article: Lallemant L, Lebreton C, Garfa-Traoré M. Comparison of different clearing and acquisition methods for 3D imaging of murine intestinal organoids. *J Biol Methods* 2020;7(4):e141. DOI: 10.14440/jbm.2020.334

effective for various samples [19].

In addition to sample processing, we also provide a comparison of four different methods of 3D image acquisition of cleared intestinal organoids: (1) laser scanning confocal microscopy, (2) spinning disk confocal microscopy allowing faster acquisitions, (3) two-photon microscopy allowing better penetration and minimal photo-bleaching, and (4) lightsheet microscopy for its fast acquisition, good penetration and reduced photo bleaching.

MATERIALS AND METHODS

Product references

Organoid culture

- ✓ LWRN cells: ATCC® CRL3276™ (from Dr. T. Stapenbeck, Washington University School of Medicine, St Louis, MO, USA)
- ✓ DMEM, High Glucose, GlutaMAX™Supplement: Gibco™-Thermo Fisher FR (Cat. # 61965240)
- ✓ DMEM/F12: Gibco™-Thermo Fisher FR (Cat. # 11320033)
- ✓ Advanced DMEM/F12: Gibco™-Thermo Fisher FR (Cat. # 12634028)
- ✓ Penicillin/Streptomycin: Gibco™-Thermo Fisher FR (Cat. # 15140122)
- ✓ Foetal Bovine Serum (FBS): Gibco™-Thermo Fisher FR
- ✓ Geneticin G418: Gibco™-Thermo Fisher FR (Cat. # 10131035)
- ✓ Hygromycin: Sigma-Aldrich FR (Cat. # H7772)
- ✓ Glutamine: Gibco™-Thermo Fisher FR (Cat. # A2916801)
- ✓ TriplExpress: Gibco™-Thermo Fisher FR (Cat. # 12605036)
- ✓ Matrigel®: Corning (Cat. # 354230)
- ✓ Phosphate-Buffered Saline without calcium or magnesium (DPBS): Gibco™-Thermo Fisher FR (Cat. # 14190-144)
- ✓ 1.4Dithiotreiol (DTT): Roche FR (Cat. # 10708984001)
- ✓ Ethylenediaminetetraacetic acid (EDTA): Sigma-Aldrich FR (Cat. # E6758)

Immunostaining

- ✓ Paraformaldehyde 36%: Electron microscopy Sciences FR (Cat. # 15714)
- ✓ BSA (Bovin Serum Albumin): Sigma-Aldrich FR (Cat. # A7906)
- ✓ Triton X-100: Sigma-Aldrich FR (Cat. # 93443)
- ✓ Antibody diluent: Life Technologies FR (Cat. # 003218)
- ✓ Monoclonal mouse Anti-sucrase-isomaltase antibody: Sigma-Aldrich FR (Cat. # WH0006476M1)
- ✓ Goat Anti-Mouse-Alexa-Fluor 488: Abcam FR (Cat. # ab 150113)
- ✓ Phalloidin Alexa-Fluor 568: Invitrogen FR (Cat. # A12380)
- ✓ NucBlue™ Fixed Cell Stain Ready Probes ™(DAPI): Invitrogen FR (Cat. # R37606)

Clearing

- ✓ RapiClear 1.47: Nikon FR (Cat. # 2SUN0001)
- ✓ N-Methyl-D-glucamine: Sigma-Aldrich FR (Cat. # U5378)
- ✓ Iohexol (Nicodenz): Proteogenix FR (Cat. # 1002424)
- ✓ 2,2′-thiodiethanol: Sigma-Aldrich FR (Cat. # 88561)
- ✓ Quadrol (N,N,N′,N′-Tetrakis ((2-Hydroxypropyl)ethylenediamine): Sigma-Aldrich FR (Cat. # 122262)
- ✓ Urea: Sigma-Aldrich FR (Cat. # U5378)
- ✓ Triton X-100: Sigma-Aldrich FR (Cat. # 93443)
- ✓ Sucrose: Sigma-Aldrich FR (Cat. # S7903)
- ✓ Triethanolamine: Sigma-Aldrich FR (Cat. # 90279)

Mounting

- ✓ IBIDI® µ-Slide 8 well: IBIDI cells in focus, 80821
- ✓ BRAND® cavity slides (L × W76 mm × 26 mm, thickness 1.2–1.5 mm, 1 concavity): Merck, BR475505-50EA
- ✓ Ligthsheet Z.1 Capillary: Zeiss product sold with Ligthsheet Z.1 microscope
- ✓ Twinsil® Speed picodent: Rotec (Cat. # 1 300 1002)
- ✓ Low-melting agarose: Sigma-Aldrich FR (Cat. # 9045)

Intestinal organoids obtaining

All mice used in the following protocol were kept in specific pathogen-free conditions.

Culture medium preparation

Seeding L-WRN cells for L-WRN medium obtaining:

1. Day 0: L-WRN cells cultured in 25 ml of "L-Cell medium" (DMEM, High Glucose, GlutaMAX™ Supplement + 10% Foetal Bovine Serum (FBS) + Penicillin/Streptomycin) in 150 cm^2 flask.
2. Day 1: Addition of Geneticin G418 (500 µg/ml) and hygromycin (500 µg/ml) to the "L-Cell medium".
3. Day 5: When the confluence is reached, cells are washed with 20 ml of PBS1X and peeled off with 1 ml of TriplExpress. After detachment, cells are re-suspended in 12 ml of "L-Cell medium".

Production of L-WRN50% conditioned medium (from Myoshi Nature protocol 2013):

1. Addition of 113 ml of "L-Cell Medium" to the 12 ml L-WRN cell suspension, and division into 5 flasks of 150 cm^2 (25 ml/flask, at 37°C and 5% CO_2).
2. After 4 d, when the confluence is reached, cells are washed with 10 ml of "Primary Culture medium" (Advanced DMEM/F12 + 20%FBS + Penicillin/Streptomycin + Glutamine).
   - 2.1. Addition of 25 ml per vial of "Primary Culture medium" and incubation at 37°C and 5% CO_2 during 24 h.
   - 2.2. Medium is collected in 50 ml tubes and 25 ml fresh "Primary Culture medium" is added to each flask.
   - 2.3. Centrifugation of the 50 ml tubes at 2000 *g* during 5 min and collection of the supernatant in a sterile 1 L bottle (approximately 125 ml). This medium is kept at 4°C.
   - 2.4. Each 24 h, medium from the same flask is collected during 4 d.
   - 2.5. After the fourth collection, addition of an equal volume (500 ml) of "Primary Culture medium" (final concentration: 50%).
   - 2.6. The "L-WRN50% medium" is well mixed, split in several 50 ml tubes and kept at −20°C until use.

Crypts isolation and organoid obtaining

Small intestine extraction: Mouse abdomen is washed with ethanol 70% and opened for small intestine extraction. Small intestine is flushed with pre-cooled Phosphate-Buffered Saline without calcium or magnesium (PBS0) and cut longitudinally with scissors into small pieces of 2 mm.

Small intestine digestion:

1. Small pieces of SI are put in pre-cooled 10 mM dithiothreitol (DTT) in PBS1X during 10 s and in 8 mM ethylenediaminetetraacetic acid (EDTA) in PBS1X, on ice, during 1 h (stirring vigorously every 15 min).
2. The supernatant is removed and pre-cooled PBS1X is put on small pieces of small intestine and vigorously pipetted using 10 ml pipette to shake tissue fragments.
3. After sedimentation, the supernatant is collected in a clean 50 ml tube and centrifuged at 70 *g* for 5 min.
4. The pellet is homogenized in 5 ml of DMEM/glutamax and crypts are counted in 20 µl DMEM by light microscopy.
5. Crypts are centrifuged at 200 *g* during 5 min and the pellet is taken in Matrigel®.

Organoid obtaining:

1. Re-suspension of the pellet of crypts in 400 µl Matrigel®, and seeding in a pre-warmed IBIDI® µ-Slide 8-well (50 µl per well).
2. Incubation at 37°C, 5% CO_2 during 10 min to allow Matrigel® polymerization.
3. Addition of 300 µl conditioned LWRN-50% medium.
4. Fresh medium is changed every 3 d and organoids are passed every 7 d.

Immunostaining and clearing

Each immunostaining and clearing step was done directly in IBIDI® µ-Slide 8-wells used to cultivate organoids.

Immunostaining

Fixation: 4% Paraformaldehyde (PFA) in PBS1X, at 37°C during 30 min.

Washing: PBS1X + 0.1% BSA, at room temperature, 3 × 5 min.

Permeabilisation: PBS1X + 0.1% Triton X-100 + 0.1% BSA, at room temperature during 10 min.

Blocking: PBS1X + 3% BSA, at room temperature during 30 min.

Immunostaining:

1. Enterocytes borders staining.
   1.1. Monoclonal mouse Anti-sucrase-isomaltase antibody (dilution 1/100) in antibody diluent at 37°C during 1 h.
   1.2. Washing: PBS1X + 0.1% BSA, at room temperature, 2 × 5 min.
   1.3. GoatAnti-Mouse-AF488 secondary antibody (dilution 1/100) in antibody diluent at 37°C during 30 min.
   1.4. Washing: PBS1X + 0.1% BSA, at room temperature, 2 × 5 min.
2. Cytoskeleton staining.
   2.1. Phalloidin-AF568 (concentration 6 µM) in antibody diluent at 37°C during 30 min.
   2.2. Washing: PBS1X + 0.1% BSA, at room temperature, 2 × 5 min.
3. Nucleus staining.
   3.1. DAPI: NucBlue™ (dilution 2 drops/ml) in PBS1X, at room temperature during 5 min.
   3.2. Washing: PBS1X at room temperature, 2 × 5 min.

Clearing

All clearing methods were done by adding 200 µl of solution in IBIDI® µ-Slide 8-wells used to grow organoids.

TDE (2,2′-thiodiethanol):

1. After immunostaining: 30%, 60%, 80% TDE in PBS1X, at room temperature during 1 d each.
2. Keep in 80% TDE until imaging.

CUBIC:

1. After fixation: Reagent-1 (Mixture of Urea (25 wt% final concentration), Quadrol (25 wt% final concentration), Triton X100 (15 wt% final concentration) and dH_2O (from Susaki *et al*., 2015 [18], at 37°C during 4 h.
2. Washing: PBS1X, at room temperature under low agitation: 2 h, overnight, 2 h.
3. Immunostaining.
4. Reagent-2 (Mixture of Urea (25 wt% final concentration), Sucrose (50 wt% final concentration), Triethanolamine (10 wt% final concentration) and dH_2O (from Susaki *et al*., 2015 [18], at 37°C during 4 h and then at room temperature until imaging.

RapiClear: After immunostaining: RapiClear 1.47 at room temperature at least for a few hours and until imaging.

Opticlear: After immunostaining: Opticlear (20% (wt/vol) N-methyl-D-glucamine, 32% (wt/vol) Iohexol (Nicodenz) and 20.48% (vol/vol) TDE, pH between 7 to 8 adjusted with hydrochloric acid (from Lai *et al*. [17]) at room temperature at least overnight and until imaging.

Mounting

Different mounting were used to image organoids.

IBIDI® µ-Slide 8-wells: The same IBIDI slide was used for the growth, clearing and imaging of organoids. 200 µl of clearing medium was added into the wells.

BRAND® cavity slide: The organoids were moved from the IBIDI® µ-Slide to the BRAND® cavity slide by gently pipetting them under excitation by an UV lamp to visualize the Dapi staining because it is very complicated to see the organoids after clearing. Fifty microlitres of clearing medium was added into the cavity and a coverslip was placed and sealed with Twinsil® Speed picodent.

Ligthsheet Z.1 capillary: the clearing medium in the IBIDI® µ-Slide used to grow and clear the organoids was removed. For uncleared organoids, the organoid was collected and transferred into a tube containing 4% low-melting agarose in PBS1X. The organoid was then aspirated into the capillary which contained approximately 50 µl of medium. We proceeded in the same way for the cleared organoid but the tube contained 4% low-melting agarose in TDE 60%. The capillary was stored at 4°C during few hours to let the mounting medium solidify.

Imaging

Laser scanning confocal microscope (LSM700 Zeiss): Images were acquired with a Plan Apochromat 20X/0.8 dry objective and with Zen Black software.

Spinning disk confocal microscope (Zeiss): The system is composed of a Yokogawa CSU-X1 spinning disk scanner coupled to a Zeiss Observer Z1 inverted microscope and controlled by Zen Blue software. Images were acquired with a Plan Apochromat 20X/0.8 dry objective through a Hamamatsu Orca Flash 4.0 sCMOS Camera.

Two-Photon microscope (TriM Scope LaVision BioTec): equipped with a Mai Tai HP SpectraPhysics Ti:Sa laser. Images were acquired with a XLUMPlanFl 20X/0.95 objective and with Imspector software.

Lightsheet microscope (Lightsheet Z1 Zeiss):

1. For non-cleared samples, the microscope imaging chamber was filled with 20 ml of water and acquisitions were done

using 10X illumination objectives and Plan Aprochromat 20X water immersion objective (NA 1.0).

2. For samples cleared with RapiClear and TDE, the microscope imaging chamber was filled with 20 ml of 80% TDE (refractive index ≈ 1.47) and acquisitions were done using LSFM 10X illumination objectives and Clr PlanNEOFLUAR 20X/1.0 corr n_d = 1.45 objective. The correcting ring was adjusted at 1.47.
3. For samples cleared with CUBIC, the microscope imaging chamber was filled with 20mL of Reagent-2 (refractive index ≈ 1.48) and acquisitions were done using LSFM 10X illumination objectives and Clr Plan–NEOFLUAR 20X/1.0 corr n_d = 1.45 objective. The correcting ring was adjusted at 1.48.

Software

Fiji was used to evaluate the "clearing ratio" (Region of Interest drawing and average pixel intensity measurements) and Imaris was used for 3D reconstruction.

RESULTS

Comparison of intestinal organoids transparency after different clearing methods

We first obtained mouse intestinal organoids following the protocol from Sato *et al*. [1,20]. After 14 d of culture in matrigel, organoids showed a dark and dense lumen in their center and several crypts composed of enterocytes and lumen (**Fig. 1A**).

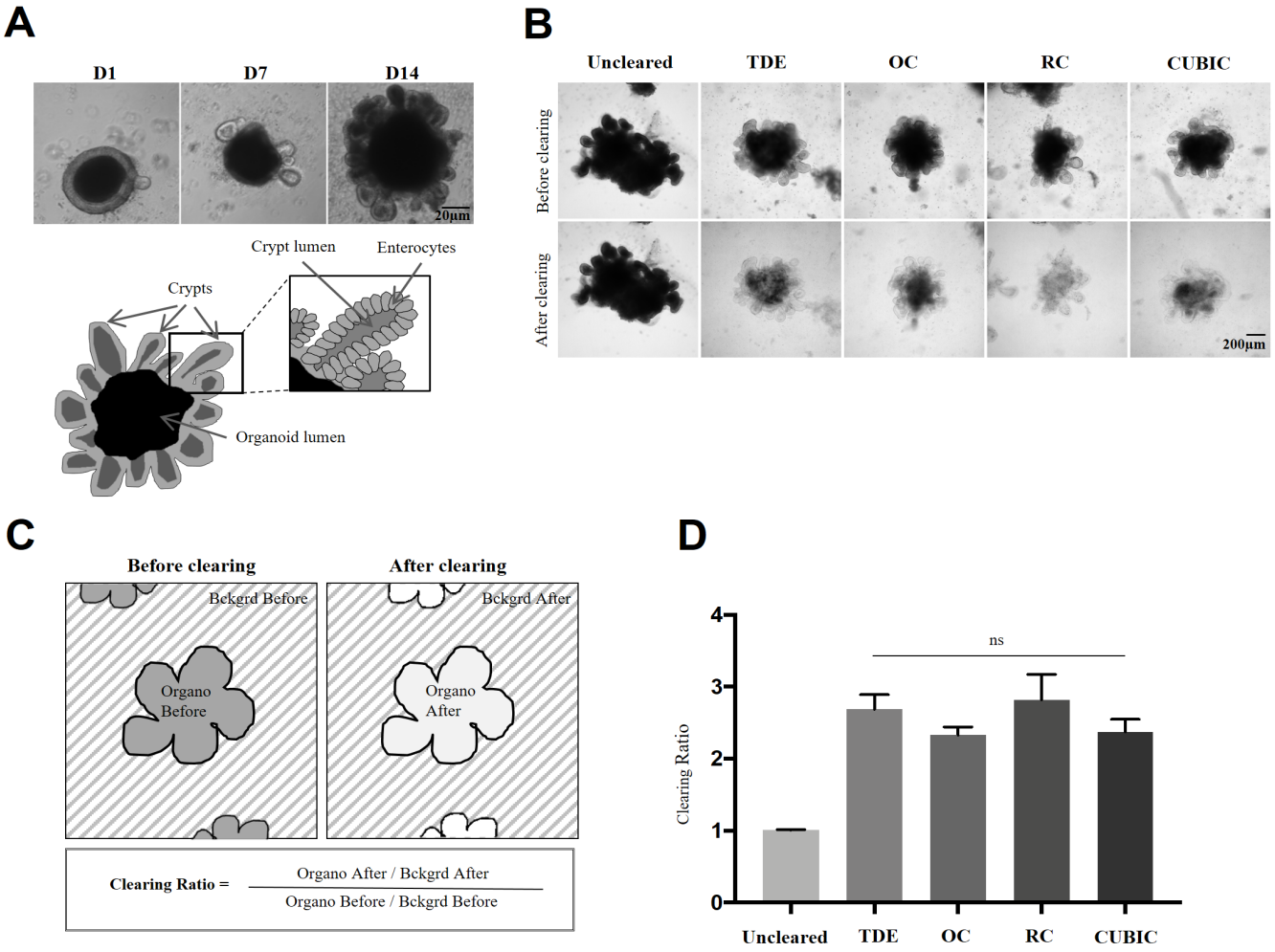

Figure 1. Comparison of intestinal organoids transparency after different clearing methods. A. Brightfield acquisitions of intestinal organoids at Day 1 (D1), Day 7 (D7) and Day 14 (D14) of culture in Matrigel and schematic representation of an organoid at D14 showing crypts, crypt lumen, enterocytes and organoid lumen. **B.** Brightfield acquisitions of approximately 800 µm thick intestinal organoids before and after different clearing methods (obj 5×, 0.16). Scale bar 200 µm for all images. **C.** Clearing ratio calculation: for each image, the average pixel intensity of the organoid (Organo) was reported to the average pixel intensity of the background (Bckgrd), then the clearing ratio was calculated by reporting the values of « After » on « Before » for each clearing methods. **D.** Analysis of clearing efficacy based on clearing ratios of brightfield acquisitions. The segmented line represents the calculated value for an uncleared sample. (*n* = 6 organoids per clearing method). Data are represented as mean ± SEM. ns: non-significant (Tukey's multiple comparisons test).

We acquired bright field images of organoids before and after clearing. We have shown that regardless of the method, the organoid became transparent after clearing, but the transparency appeared more homogenous following RapiClear clearing method (**Fig. 1B**). To quantify this observation and test the efficacy of each clearing method in terms of transparency, we calculated a clearing ratio. Clearing ratio was calculated on organoids of equivalent size. We chose only 800 µm thick organoids for all conditions so that the clearing efficiency is comparable from one sample to another independently of the thickness of the sample. For each image and clearing method, the average pixel intensity of the organoid was reported to the average pixel intensity of background before and after clearing (**Fig. 1C**). The results showed no significant difference of the clearing ratio between all methods (**Fig. 1D**). In summary, the four clearing methods tested seem equally effective.

Fluorescence preservation after different clearing methods on intestinal organoids

We then checked the fluorescence preservation after each clearing method by labeling intestinal organoids nuclei with DAPI, the enterocyte borders with sucrase-isomaltase immunofluorescence and the cytoskeleton with fluorochrome conjugated-phalloïdin (**Fig. 2A**).

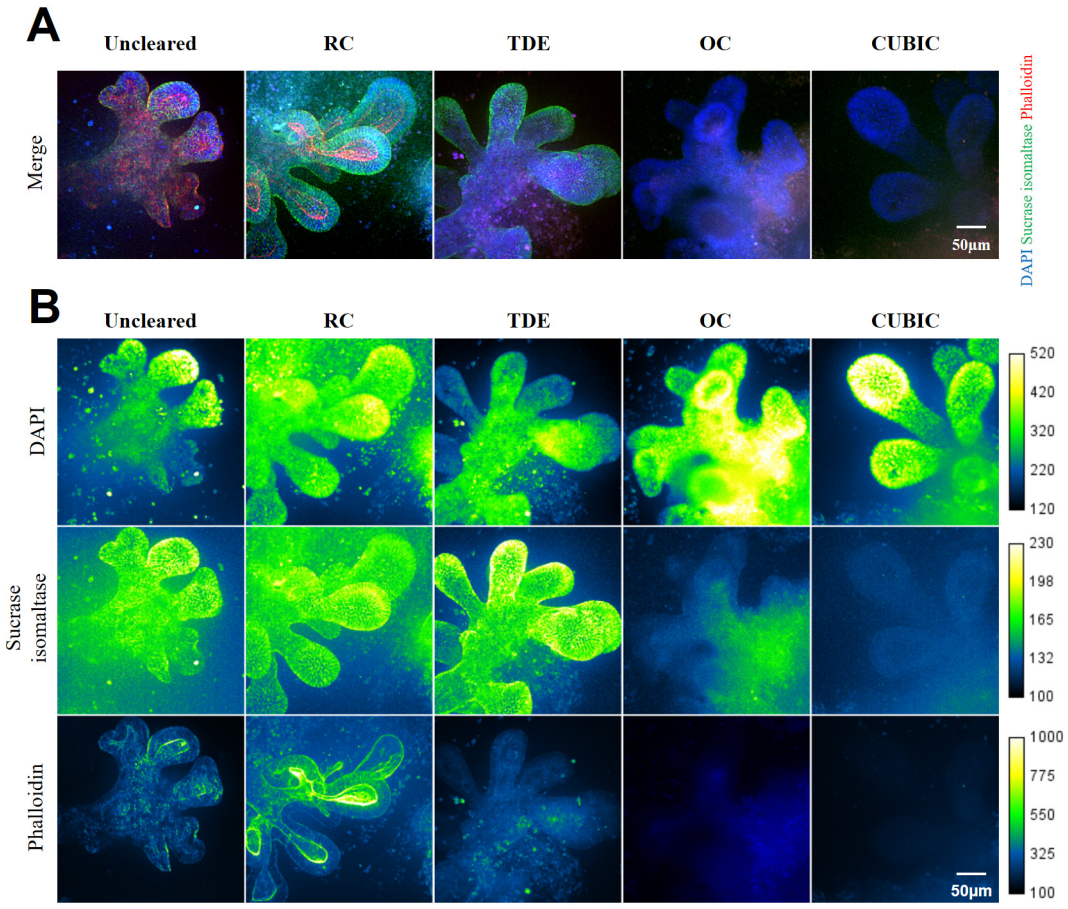

Figure 2. Fluorescence preservation after different clearing methods on intestinal organoids. A. Spinning disk acquisitions (obj 20×, NA = 0.8) of uncleared and cleared intestinal organoids with different clearing methods. DAPI (blue, λ_{ex}: 405 nm, λ_{em}: 450/50 nm), Sucrase Isomaltase (green, λ_{ex}: 488 nm, λ_{em}: 520/35 nm) and Phalloidin (red, λ_{ex}: 561 nm, λ_{em}: 630/98 nm). Scale bar 50 µm. **B.** A green fire blue color map was applied to show fluorescence intensity levels. Scale bar 50 µm.

We applied a false color to the images to better visualize the variations in intensity from one image to another. The nuclear staining was not impaired by any of the clearing methods. We found high fluorescence intensities for DAPI in all conditions. However, this was not the case for the sucrase-isomaltase labeling: the fluorescence of the enterocyte borders was lost with Opticlear and CUBIC. Concerning phalloïdin staining, it was only preserved by RapiClear and the loss was very pronounced with CUBIC and Opticlear (**Fig. 2B**). In light of these results, we conclude that the choice of the clearing technique must take into account the purpose of the experiment and the structures that are visualized by immunofluorescence.

Comparison of different acquisition modes

Finally, we compared different acquisition methods to image organoids stained with DAPI and cleared with RapiClear. Depending on the microscope, we used different mounting strategies: IBIDI®µ-Slides or BRAND® cavity slides for confocal, spinning disk and two-photon microscopy. For lightsheet microscopy, capillaries were used, combined with low-melt-

ing agarose and clearing medium to fill them in order to improve light penetration and avoid light scattering (**Fig. 3A** and **3B**. See Methods).

We first showed that confocal and spinning disk microscopes enabled the same acquisition depth (200 µm) but the spinning disk microscope was 4 times faster. Two-photons and lightsheet microscopy allowed deeper acquisitions (800 µm), when compared to confocal and spinning disk microscopes. Lightsheet acquisition had the additional advantage of being 30 times faster than the two-photon microscope (**Fig. 3B**).

Importantly 3D reconstruction was possible using these four different acquisition methods. However, only two-photon and lightsheet microscopy allowed to visualize the entire organoid, and throughout its full thickness (**Fig. 3C**).

A

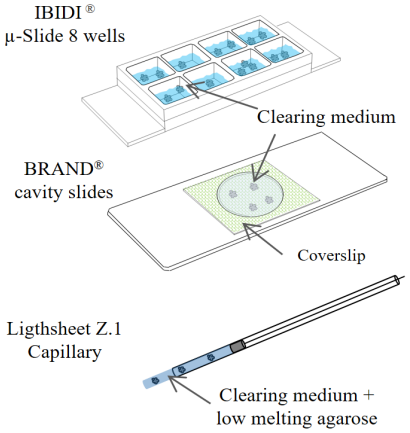

B

	Confocal	Spinning Disk	2-photons	Ligthsheet Z1
Mounting	IBIDI® µ-Slide 8 wells or BRAND® cavity slides	IBIDI® µ-Slide 8 wells or BRAND® cavity slides	IBIDI® µ-Slide 8 wells or BRAND® cavity slides	Ligthsheet Z.1 Capillary
Acquisition depth	≈ 200µm	≈ 200µm	≈ 800µm	≈ 800µm
Acquisition time for 100 µm	4min	1min	5min	10sec

C

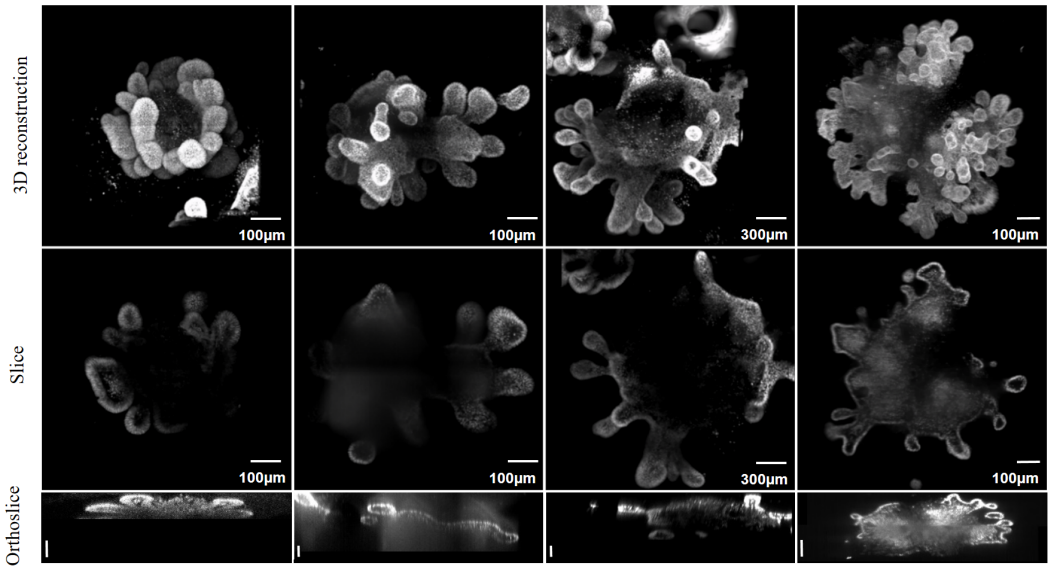

Figure 3. Comparison of different acquisition methods. A. Different mounting methods for acquisitions. IBIDI® µ-Slides or BRAND® cavity slides for confocal, spinning disk and two-photon microscopy. For lightsheet microscopy, capillaries were used in combination with low-melting agarose and clearing medium to fill them in order to improve the light penetration and avoid light scattering. **B.** Comparison of the mounting methods, the acquisition depth and acquisition time for different microscopy approaches. **C.** 3D reconstruction, slice and orthogonal view of representative acquisitions of intestinal organoids stained with DAPI (λ_{ex}: 405 nm, λ_{em}: 450/50 nm, Zstep: 0.44 µm), cleared with RapiClear, and imaged in BRAND® cavity slides (for confocal, spinning disk and two-photon) or lightsheet Z.1 capillary. Vertical scale bar = 50 µm.

DISCUSSION

Biological tissues are composed of heterogeneous materials with different optical properties, limiting deep observation due to light scattering and absorption. The development of clearing methods to reduce light scattering by homogenization of refractive index allowed the observation and imaging of thick samples in their entirety.

Using whole mouse intestinal organoids as a model system, we

sought to compare four different clearing methods previously described in the literature, and investigated to which extent they allowed organoid imaging without the need of challenging techniques of organoid sectioning. These clearing methods have first been developed for large organs such as the mouse brain but can be applied to small specimens, like organoids. There are, however, a wide variety of methods which can be classified into four families depending of the clearing agents used: organic solvents, high refractive index aqueous solutions, hyperhydrating solutions and hydrogel embedding. The choice of method is determined by the size of the sample and the need for subsequent immunofluorescent labelling.

In our study, we compared simple immersion methods in aqueous solutions with high refractive index (TDE, RapiClear and Opticlear) as well as a hyperhydration method (CUBIC) because they are easy to implement and inexpensive.

Intestinal organoids are composed of different parts, such as crypts, epithelial cells and a very dark and dense center, with different optical properties. We have shown that these four clearing methods offer the same transparency efficacy based on the calculation of a clearing ratio. However, RapiClear, a commercial product whose composition is unknown, allows better homogenization of the clearing. We hypothesize that one of the components of this clearing agent allows better penetration and better diffusion of the solvent into the sample.

We have tested RapiClear on other types of organoids, such as cerebellar organoids, with good clearing efficiency (Data not shown). This commercial solution can therefore be used on other types of organoids.

Our next step was to label the organoid structures and assess the effect of the clearing medium on the fluorescence. We decided to test intercalating fluorescent dyes such as DAPI and phalloïdin and an immunofluorescence labelling, sucrase-isomaltase, which is found on the surface of cells. We have chosen these targets to avoid potential complications of antibody penetration.

According to our results, RapiClear preserves at best the fluorescent labelling, adding an extra advantage of this method to the extensive homogenisation of the clearing. TDE retains fluorescent labelling with the exception of phalloïdin. Given the high cost of RapiClear, TDE can offer an alternative and an inexpensive solution. Despite several reports on their ability to retain fluorescence [17,18], our results do not support the use of CUBIC and Opticlear for the study of intestinal organoids.

The last important step for 3D imaging of cleared sample is the choice of an adapted imaging technique. We compared four microscopy approaches. Our results showed that the Zeiss ligthsheet Z1 microscope is the best solution for quick and deep acquisitions of intestinal organoids. Since ligthsheet microscopy is not widely available, other more common methods of image acquisition may be sufficient to study intestinal organoids.

In summary, using mouse intestinal organoids as a model system, we conclude that RapiClear-based clearing in association with lighsheet image acquisition yields the best results and allows rapid and deep visualization of the sample in its entirety.

Acknowledgments

The authors thank Dr. Nadine Cerf-Bensussan for providing the equipment needed for sample preparation. They thank Dr. Mario Gomes-Pereira and Soumaiya Imarraine for critical reading of the manuscript.

References

1. Sato T, Clevers H (2013) Primary mouse small intestinal epithelial cell cultures. Methods Mol Biol 945: 319-328. doi: 10.1007/978-1-62703-125-7_19. PMID: 23097115
2. Sato T, Vries RG, Snippert HJ, van de Wetering M, Barker N, et al. (2009) Single Lgr5 stem cells build crypt-villus structures in vitro without a mesenchymal niche. Nature 459: 262-265. doi: 10.1038/nature07935. PMID: 19329995
3. Spence JR, Mayhew CN, Rankin SA, Kuhar MF, Vallance JE, et al. (2010) Directed differentiation of human pluripotent stem cells into intestinal tissue in vitro. Nature 470: 105-109. doi: 10.1038/nature09691. PMID: 21151107
4. Kretzschmar K, Clevers H (2016) Organoids: modeling development and the stem cell niche in a dish. Dev Cell 38: 590-600. doi: 10.1016/j.devcel.2016.08.014. PMID: 27676432
5. Zhang R, Koido M, Tadokoro T, Ouchi R, Matsuno T, et al. (2018) Human iPSC-derived posterior gut progenitors are expandable and capable of forming gut and liver organoids. Stem Cell Reports 10: 780-793. doi: 10.1016/j.stemcr.2018.01.006. PMID: 29429958
6. Nigro G, Hanson M, Fevre C, Lecuit M, Sansonetti PJ (2016) Intestinal organoids as a novel tool to study microbes–epithelium interactions. In: Turksen K. (eds) Organoids. Methods in molecular biology, vol 1576. New York: Humana. doi: 10.1007/7651_2016_12.
7. Fasciano AC, Mecsas J, Isberg RR (2019) New age strategies to reconstruct mucosal tissue colonization and growth in cell culture systems. Microbiol Spectr 7. doi: 10.1128/microbiolspec.BAI-0013-2019. PMID: 30848233
8. Dedhia PH, Bertaux-Skeirik N, Zavros Y, Spence JR (2016) Organoid models of human gastrointestinal development and Disease. Gastroenterology 150: 1098-1112. doi: 10.1053/j.gastro.2015.12.042. PMID: 26774180
9. Sato T, Clevers H (2015) SnapShot: growing organoids from stem cells. Cell 161: 1700-1700. doi: 10.1016/j.cell.2015.06.028. PMID: 26091044
10. Nagaishi K, Arimura Y, Fujimiya M (2015) Stem cell therapy for inflammatory bowel disease. J Gastroenterol 50: 280-6. doi: 10.1007/s00535-015-1040-9. PMID: 25618180
11. Vigouroux RJ, Belle M, Chédotal A (2017) Neuroscience in the third dimension: shedding new light on the brain with tissue clearing. Mol Brain 10: 33. doi: 10.1186/s13041-017-0314-y. PMID: 28728585
12. Dekkers JF, Alieva M, Wellens LM, Ariese HCR, Jamieson PR, et al. (2019) High-resolution 3D imaging of fixed and cleared organoids. Nat Protoc Jun 14: 1756-1771. doi: 10.1038/s41596-019-0160-8. PMID: 31053799
13. Tainaka K, Kuno A, Kubota SI, Murakami T, Ueda HR (2016) Chemical principles in tissue clearing and staining protocols for whole-body cell profiling. Annu Rev Cell Dev Biol 32: 713-741. doi: 10.1146/annurev-cellbio-111315-125001.
14. Silvestri L, Costantini I, Sacconi L, Pavone FS (2016) Clearing of fixed tissue: a review from a microscopist's perspective. J Biomed Opt 21: 81205. doi: 10.1117/1.JBO.21.8.081205. PMID: 27020691
15. Richardson DS, Lichtman JW (2015) Clarifying tissue clearing. Cell 162: 246-257. doi: 10.1016/j.cell.2015.06.067. PMID: 26186186
16. Aoyagi Y, Kawakami R, Osanai H, Hibi T, Nemoto T (2015) A rapid optical clearing protocol using 2,2′-thiodiethanol for microscopic observation of fixed mouse brain. PLoS One 10: 1. PMID: 25633541
17. Lai HM, Liu AKL, Ng HHM, Goldfinger MH, Chau TW, et al. (2018) Next generation histology methods for three-dimensional imaging of fresh and archival human brain tissues. Nat Commun 9: 1066. doi: 10.1038/s41467-018-03359-w. PMID: 29540691
18. Susaki EA, Tainaka K, Perrin D, Yukinaga H, Kuno A, et al. (2015) Advanced CUBIC protocols for whole-brain and whole-body clearing and imaging. Nat Protoc [Internet 10: 1709-1727. doi: 10.1038/nprot.2015.085. PMID: 26448360
19. SunJin Lab (2015) One-step tissue clearing: Visualize 3D architecture of tissue with ease. Available from: https://www.sunjinlab.com/wp-content/uploads/One_Step_Tissue_Clearing_Reagents.pdf
20. Sato T, Stange DE, Ferrante M, Vries RGJ, Van Es JH, et al. (2011) Long-term expansion of epithelial organoids from human colon, adenoma, adenocarcinoma, and Barrett's epithelium. Gastroenterology 141: 1762-1772. doi: 10.1053/j.gastro.2011.07.050. PMID: 21889923